Nanoscale

Accepted Manuscript

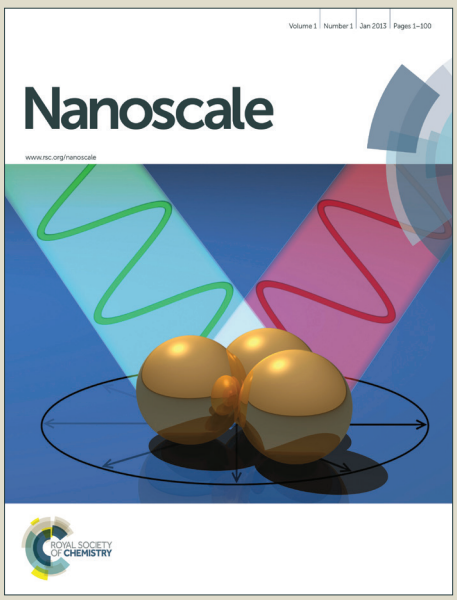

ROYAL SOCIETY OF CHEMISTRY

www.rsc.org/nanoscale

Journal Name

RSCPublishing

ARTICLE

Magnonic gas sensor based on mangnetic nanoparticles

Cite this: DOI: 10.1039/x0xx00000x

D. Matatagui[a], O.V. Kolokoltsev[a], N. Qureshi[a], E.V. Mejía-Uriarte[a], J.M. Saniger[b]

Received 00th January 2012,
Accepted 00th January 2012

DOI: 10.1039/x0xx00000x

www.rsc.org/

In this paper, we propose an innovative, simple and inexpensive gas sensor based on the variation of the magnetic properties of nanoparticles due to their interaction with gases. To measure the nanoparticles response a magnetostatic spin wave (MSW) tunable oscillator has been developed using an yttrium iron garnet (YIG) epitaxial thin film as a delay line (DL). The sensor has been prepared by coating a uniform layer of $CuFe_2O_4$ nanoparticles on the YIG film. The unperturbed frequency of the oscillator is determined by a bias magnetic field, which is applied parallel to the YIG film and perpendicularly to the wave propagation direction. In this device, the total bias magnetic field is the superposition of the field of a permanent magnet and the field associated with the layer of magnetic nanoparticles. The perturbation produced in the magnetic properties of the nanoparticle layer due to it interaction with gases induces a frequency shift in the oscillator, allowing the detection of low concentrations of gases. In order to demonstrate the ability of the sensor to detect gases, it has been tested with organic volatile compounds (VOCs) which have harmful effects on human health, such as, dimethylformamide, isopropanol and ethanol, or the aromatic hydrocarbons like benzene, toluene and xylene more commonly known by its abbreviation (BTX). All of these were detected with high sensitivity, short response time, and good reproducibility.

1. Introduction

An important issue revolves around the potential uses of volatile organic compounds (VOCs) in industry and in household goods, which may lead to serious medical and environmental problems. Some significant VOCs are highlighted benzene, toluene and xylene (BTX), since exposure to BTX may result in the occurrence of cancer and other adverse health effects[1-4].

Due to many of the acute toxicities of the VOCs, there has been an increasing need for developing new sensitive, low-cost and portable systems, which can respond in real time, for monitoring trace levels of VOCs in various environmental and industrial applications. Many works have led to innovative systems to detect VOCs such as chromatography[5], ion mobility spectrometry[6], Raman spectroscopy[7], etc. Though these detectors are accurate, they can be bulky and expensive, and require highly-qualified operators. On the other hand, there are low-cost devices, with high sensitivity and low dimensionality known as chemical sensors, which are based on capacitive effects[8, 9], resistive effects[10, 11], optical fibers[12, 13], field effect transistors (FETs)[14, 15], surface acoustic waves (SAWs)[16, 17] and quartz crystal microbalances (QCM)[18, 19]. Many of the sensors that have been developed for specific applications in toxic chemical agent detections, are based on metal oxides, since they are relatively easy to fabricate, and have low detection limits. Metal oxides have been, in most cases, sensitive layers used for development of resistive sensors, which have become a prime technology in several domestic, commercial, and industrial gas detection systems. Among the more important metal oxides used in sensors are: WO_3[20], NiO[21], SnO_2[10], $In2O_3$[22], TiO_2[23], ZnO[24], CuO_2 and CuO[25]. However, resistive sensors based on metallic oxides have a major disadvantage: they posses great sensitivity at high temperatures but a poor sensitivity at room temperature.

Among metal oxides, magnetic materials have also been used to detect gases[26-28]. However, only a few experimental studies have been reported on the perturbation of magnetic properties caused by an interaction of gases[29]. In contrast with resistive properties, the perturbation of magnetic properties are more pronounced at low temperatures, which is an important advantage for their application in gas sensor technology.

A relatively slow advance in the development of magnetic chemical sensors, is apparently due to the absence of inexpensive solutions for accurately measuring weak variations induced in magnetic characteristics of the sensitive material. In this work we show that tunable magnetostatic spin wave (MSW) oscillators possess a more than sufficient sensitivity to register these induced variations. Devices known as YIG sphere oscillators based on yttrium iron garnet (YIG) have been used for more than fifty years in microwave instruments. The developement of planar spin-wave technology has led to the apearence of thin-film oscillators based on magnetostatic surface waves (MSSW) [30, 31]. In the context of this work the

advantage of thin-film MSSW devices over the volumetric YIG sphere oscillators is that the planar spin-wave element, a delay line (DL), can be easily coated with sensitive magnetic layers. Among properties of MSSWs, it is important to point out their very low propagation losses at microwave frequencies, high loaded Q value, small wavelength and high tuneability (from 0.2 GHz up to 20 GHz). It should be noted that, the frequency of a spin-wave oscillator can be tuned by changing the magnitude of a bias magnetic field, while the MSSW wavelength remains constant. Consequently, numerous novel devices and applications based on MSW oscillators have been recently demonstrated [32-35].

Based on these considerations, an idea enabling a new generation of chemical sensors is the combination of an MSSW oscillator as a magnetic field detector, with a layer of magnetic nanoparticles of $CuFe_2O_4$ as a sensitive layer for gas sensors. We call this concept a "magnonic gas sensor": a chemical sensor based on the change of magnetic properties, which are measured by a MSSW oscillator. A sensitive magnetic material has been used in the form of nanoparticles in order to create very large surface-to-volume ratio that can significantly increase the sensitivity.

2. Experimental

2.1. Magnetostatic surface wave oscillator

The MSW oscillator was based on a 4 mm x 2 mm rectangular ferromagnetic sample, composed of a 7.3 µm thick YIG film on a 0.5 mm thick gallium gadolinium garnet (GGG) substrate (Fig. 1a). By placing two microstrip-line antennas over the YIG film, a two-port delay line was formed. The width of the two coupling antennas was 0.5 mm, and the spacing between the antennas was 3 mm (Fig. 1b). In our case, a bias magnetic field (H_B), applied perpendicularly to the wave propagation direction and parallel to the YIG film plane, gives rise to MSSW propagation along the largest dimention of the sample. The typical wavelength of MSSW was ≈500µm. This MSSW-DL was introduced into the feedback loop of a solid-state amplifier and a directional coupler, satisfying the criteria for oscillation: the total phase shift in the loop is 2πn (n = integer), and the gain over the closed loop is 1 (Fig. 1c). The oscillation frequency of the device (f) can be aproximated by:

$$f = f_0 + \delta f_{SL} = \gamma(H_B + H_{SL}) + \gamma\delta H_{SL}$$

where f_0 is the unperturvated oscillation frequency, δf_{SL} is the frequency shift due to the interation between the sensitive layer and the toxic gas, $\gamma \approx 2.8$ MHz/Oe is the gyromagnetic constant, H_{SL} is the static magnetic field to be induced by a sensitive layer and δH_{SL} is the variation of magnetic field induced by the interation between the sensitive layer and the toxic gas. The coupled output from the directional coupler was used to obtain in real time a sample of the frequency from the oscillator without interrupting the main power flow.

The oscillator was tunable within a microwave frequency range of 0.2 to 3 GHz, limited by the solid-state amplifier. However, with careful control over the bias magnetic field and with a suitable amplifier, the oscillation frequency can be extended to 8 GHz. The linewidth of the generated microwave oscillations was less than 0.4 kHz.

2.2. Magnetic nanoparticles as a sensitive layer

$CuFe_2O_4$ nanopowder (Sigma 771929) with an average size of 100 nm was used as a gas sensitive layer. A dispersion of 0.17 g of $CuFe_2O_4$ nanopowder was dispersed in 1 ml of isopropanol by means of sonication for 1 h. The uniform nanoparticle dispersion was deposited by spin coating on the YIG as a film at a rate of 2000 rpm, and then a 30-minute postbake at 100ºC was carried out in order to fix the nanoparticles on the MSSW-DL and eliminate the isopropanol (Fig. 1a). The layer of nanoparticles acts as the sensing material; this is because the interaction with the volatile compounds produces a change in magnetic properties of the nanoparticles and consequently the total bias magnetic field changes and leads to a frequency shift in the oscillating device.

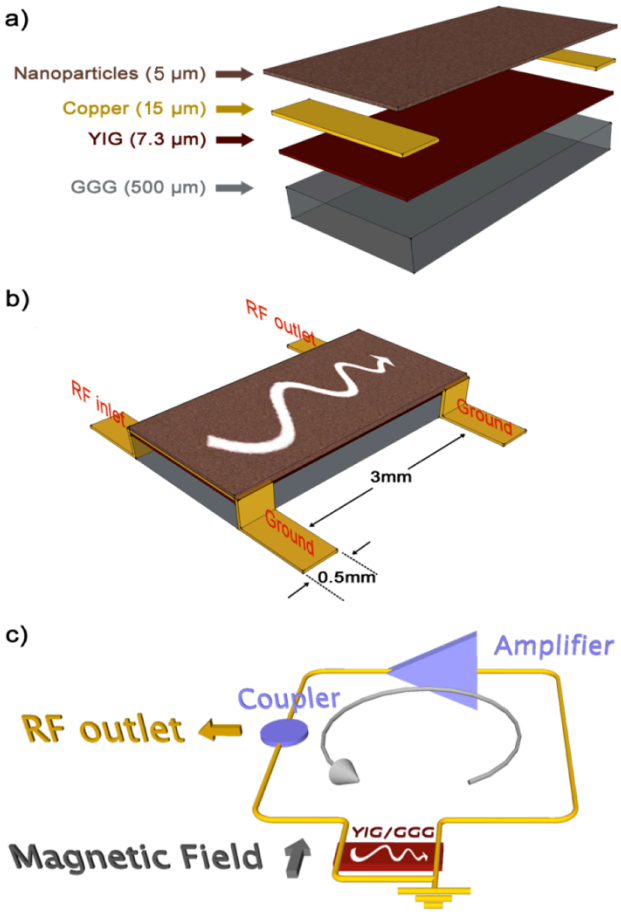

Fig. 1 Two-port MSSW-DL (a) composition layer (b) geometrical parameters. (c) Scheme of the oscillator controlled by the MSSW-DL.

2.3. Samples and experimental setup

The volatile compounds used in the experiment were: dimethylformamide, isopropanol, ethanol, benzene, toluene, xylene, and water. The vapor concentration was calculated using Antoine's Equation. The volume of the liquid samples was 5 ml (Fig. 2). They were kept at a constant temperature of 3ºC in a thermal bath for 30 minutes (headspace time) before being carried to the chamber. The volatiles were extracted and diluted with synthetic air, which was controlled by two mass flow controllers (MFC) in order to carried out the cycles of gas exposition and purge, and the desired concentration with a constant airflow in the sensor chamber of 100 ml min^{-1}. Different exposition and purge times were tested between 5 min and 1 min each, but 1 min was enough in order to detect the toxic gases and obtain a stable frequency in almost all cases. Therefore, 1 min of exposition and purge was used in order to show the fast response of the sensor. The experimental control and data acquisition in real time were implemented with a PC using custom made software.

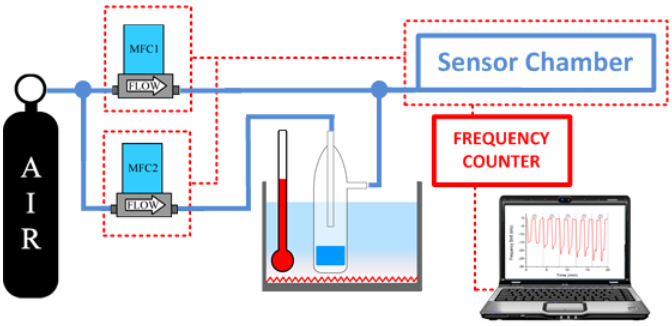

Fig. 2 Simple scheme of the instrumentation and experimental set up used for the data acquisition in real time.

3. Results and discussion

3.1. Morpological of nanoparticle layer

The thickness of the nanoparticle layer was measured through a profilometer (Dektak IID), which yielded a thickness of approximately 5 µm.

Additionally, the nanoparticle layer was studied by scanning electron microscope (SEM JSM-7800F). Fig. 3, shows a SEM image of the prepared $CuFe_2O_4$ nanoparticle layer. First, the sensitive layer was studied with magnification of x10000, showing a continuous layer of nanoparticles with high-porosity, which is important because the gases can penetrate quickly into the sensitive layer. A second study was carried out with magnification of x30000 (Fig. 3, top-left), which shows that the film was composed of nanoparticles smaller than 100 nm.

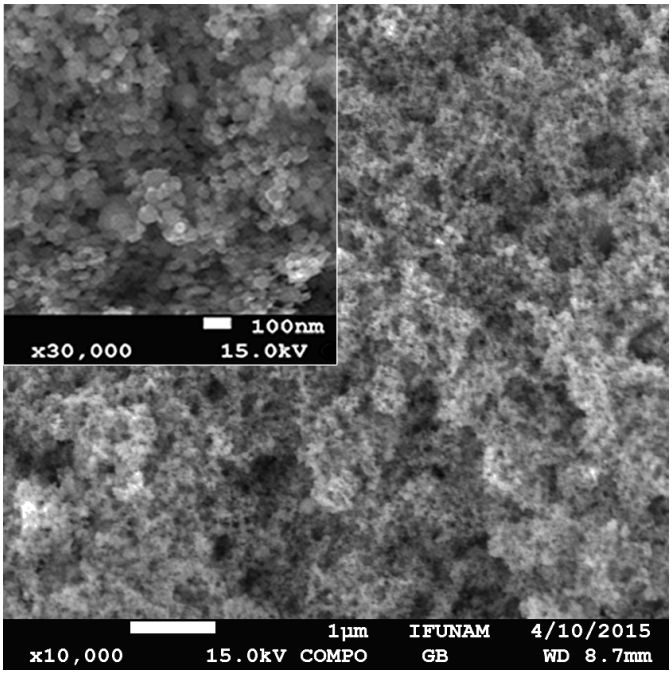

Fig. 3 SEM image of the $CuFe_2O_4$ nanoparticle layer deposited by spin coating as a gas sensitive layer. In the main image the magnification is 10000x and in the insert the magnification is 30000x.

3.2. Electrical characterization of the MSSW-DL

An Automatic Network Analyzer (Wiltron 360B) was used to measure the frequency response of the MSSW-DL. The bias magnetic field H_B was 200 Oe, resulting in MSSW propagation centred about 1 GHz (Fig. 4). The RF transmission parameter S_{21}, was then studied in three different cases: (1) without any material over YIG, (2) with a non-magnetic and dielectric layer (alumina particles) deposited on YIG, and (3) with a magnetic layer ($CuFe_2O_4$ particles) on YIG. Despite the strong difference in dielectric properties between air and alumina, the change in the frequency response S_{21} (attenuation and phase) was very small, as seen in Fig. 4. However, the presence of the ferrite layer over YIG (third case) implies an important alteration in YIG waveguide, producing strong changes in the frequency response of S_{21}. The data in Fig.4 indicate that the frequency shift of the gas sensor response, reported in this work, can be attributed to changes in magnetic properties of $CuFe_2O_4$ nanoparticles rather than their dielectric properties.

Fig. 4 also shows a linear phase of MSSW over the whole frequency range where MSSW were propagated. This means that there were no parasitic interferences in the signal transmission, resulting in a stable oscillation when the MSSW-DL was introduced into the amplifier loop.

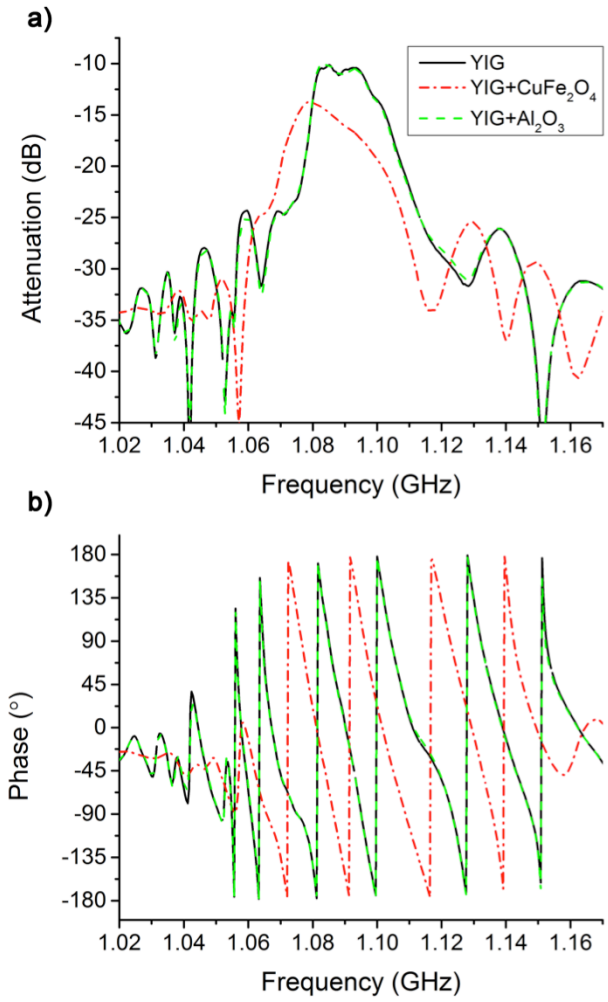

Fig. 4 Attenuation (a) and phase (b) for the transmission parameter S_{21} in different cases: solid curve (black) shows S_{21} without any material over YIG; dashed line (green) shows the response when a layer of alumina particles was deposited on YIG; dashed-dot (red) curve shows S_{21} for YIG film covered by a layer of $CuFe_2O_4$ particles.

3.3. Gas characterization

To verify that the sensor formed by combining of an MSSW-DL and a layer of $CuFe_2O_4$ nanoparticles was suitable as a gas sensor, this was tested with different concentrations of six kinds of VOCs (dimethylformamide, isopropanol, ethanol, benzene, toluene and xylene).

The gas system generator described in section 2.3 provided the range of concentrations used for each VOC. It is important to note that the lowest concentration measured for each VOC was the lowest concentration that could possibly be obtained by the gas generator system and not the detection limit of the sensor.

Testing cycles were carried out with a constant exposure and a purge of 1 min. During exposure of each concentration to the VOCs the frequency of the sensor suffered a frequency shift (δf_{SL}) toward higher values, which means that the the total magnetic field applied in the YIG increase. Then, the sensor was purged with synthetic dry air, which shifted the frequency back to the initial value, and therefore, the gas-induced magnetic changes in the nanoparticle layer were reversible, which is essential for practical sensors.

Fig. 5 shows the real time detection at room temperature for the different concentrations of each VOC, which were determined by a frequency shift much higher than noise, and with a fast response time. For instance, the DMF measured concentrations 50, 75, 100, 150, 200, 250 and 300 ppm, had a response time to reach 90% of their frequency shift final value, τ_{90}, of 49, 49, 47, 43, 40, 35 and 26 s respectively.

Fig. 6 shows the frequency shift of the sensor for each VOC. The maximum frequency shift was found to increase with higher VOCs concentrations. Ethanol, benzene and xylene showed a saturated behaviour for higher concentrations.

The repeatability of the sensor was tested in two different forms. First, each concentration was measured twice in continuous cycles, during which a similar frequency shift was obtained. Then, after detection of all VOCs, approximately one month later we repeated the measurements with 200 ppm of xylene, as a control test. These two measurements are compared in Fig. 7, showing similar values of frequency shifts in both cases. This means that all relevant physical and chemical processes in the detection were reversible, and thus sensor was free of poisoning due to the reaction with the VOCs.

Another testing experiment was conducted in order to confirm the role of the layer of $CuFe_2O_4$ nanoparticles in the sensing process. After measurements, the layer of nanoparticles was removed and the detection of xylene at 200 ppm was repeated. No frequency response was observed, confirming that the gas sensing effect result from the interaction of VOC molecules with the $CuFe_2O_4$ nanoparticle layer, inducing the concomitant increase of the total magnetic field applied in the YIG.

The change in magnetic properties of nanoparticles upon interaction with gases could be a consequence of diverse mechanisms. The magnetic properties of nanoparticles are modulated by surface effects, which results from the symmetry breaking of the nanocrystal structure at the surface of the particle, surface strain, the presence of dangling bonds or molecular species capping and stabilizing the nanoparticles, or even differences in the structure between the core and surface parts of the nanoparticle[36]. In this framework, the adsorption of a gaseous compound is an additional factor contributing to a modification in the nanoparticle surface state, which leads to a chang in its magnetic response. Different kinds of gaseous compounds, having different interactions with the nanoparticle surface, will contribute with a greater or lesser degree to the change of the nanoparticles magnetic properties.

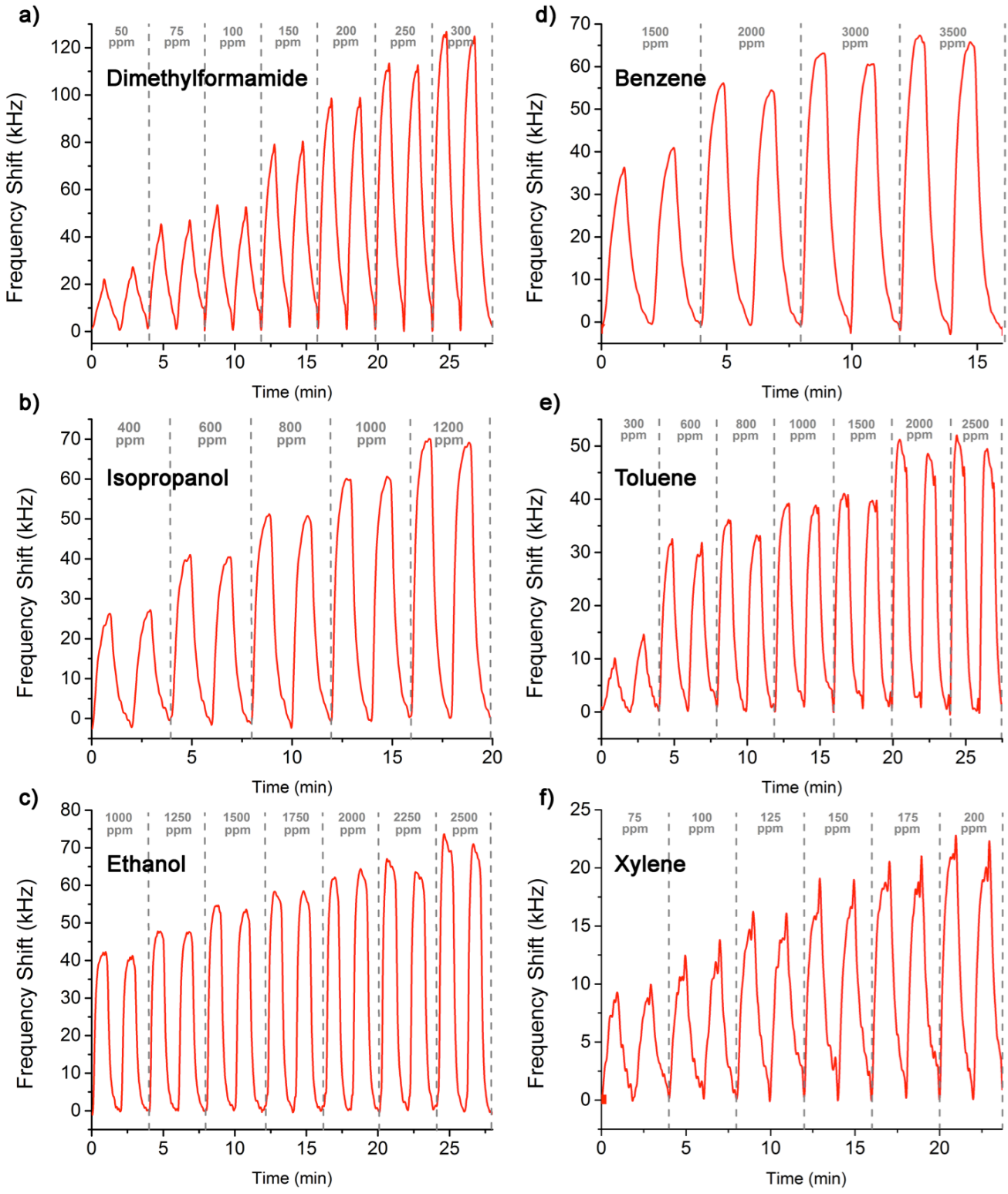

Fig. 5 Real-time response of the magnetic gas sensor at room temperature for different VOCs: (a) dimethylformamide, (b) isopropanol, (c) ethanol, (d) benzene, (e) toluene and (f) xylene, varying as a function of the concentrations in dry air. Testing cycles were carried out with constant exposure and purge of 1 min.

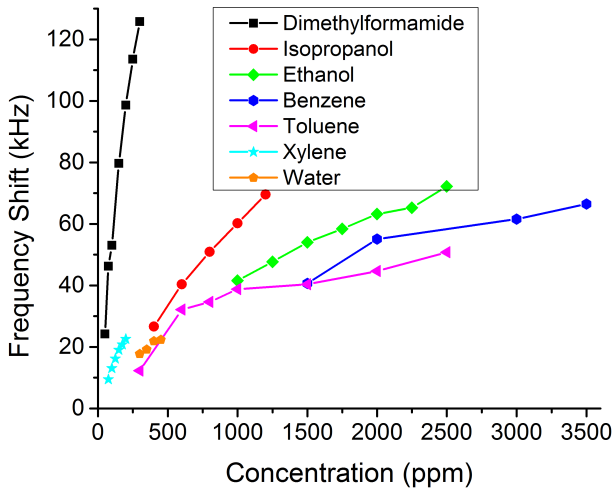

Fig. 6 Variation in the sensor response as a function of VOCs concentration. An increase in the sensor response with rising gas concentration is clearly seen. Ethanol, benzene and xylene show a saturated behaviour for the higher concentrations.

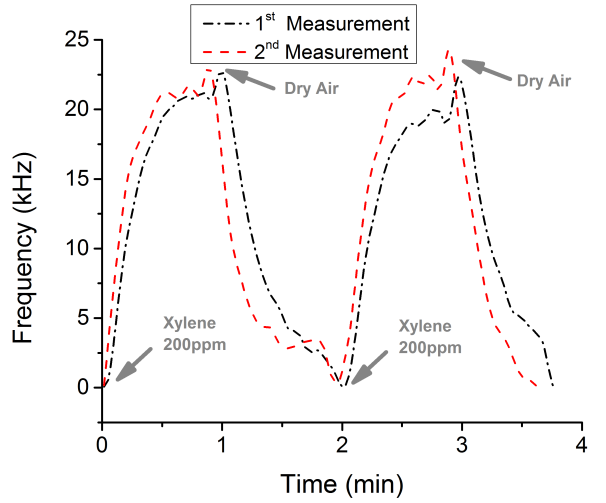

Fig. 7 Long-term repeatability of the sensor, comparing the responses to 200 ppm of xylene one month apart (1st and 2nd measurements, respectively).

An important factor in gas sensor is the detection of water, better known as "humidity sensors". Different concentrations of water in air, absolute humidity, were detected with a high sensitivity and fast response time. Fig.8 shows the case of water concentrations, for which the sensor response saturates. On one hand, in this particular case of the magnetic layer, the sensor is a good detector for low humidity concentrations. On the other hand, the frequency shift for water was comparable to frequency shift for the toxic gases used. This means that sensing of toxic gases experiences some humidity interference that has to be taken into account and minimised. For example, using humidity filters, functionalizing the nanoparticle with a hydrophobic substance or heating the sensor to moderate temperatures in order remove chemisorbed humidity could address this issue.

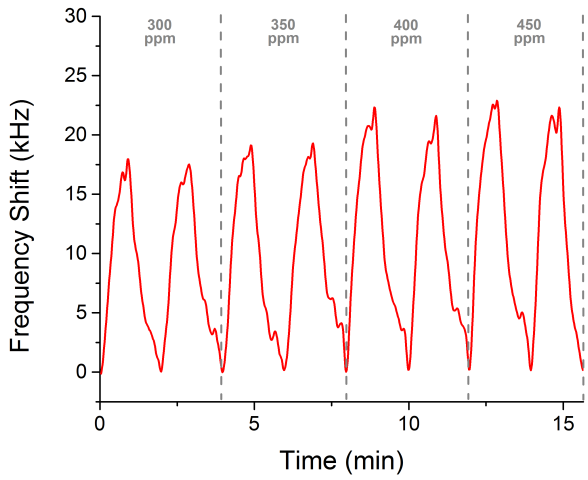

Fig. 8 Real-time response of the MSSW oscillator combined with $CuFe_2O_4$ nanoparticles for different concentrations of water vapour.

Conclusions

In summary, this paper describes an innovative, simple and inexpensive magnetic gas sensor based on the combination of magnetic nanoparticles, as a sensitive layer, and a magnetostatic surface wave oscillator as a transducer. It is shown that the magnetic nanoparticles of $CuFe_2O_4$, deposited on YIG film via the spin coating technique, can detect low concentrations of different VOCs (dimethylformamide, isopropanol, ethanol, benzene, toluene and xylene). The sensor operates at room temperature, with high sensitivity, short response time, and good reproducibility.

We believe that the solution presented opens a new and promising field of research in "nanomagnetic gas sensing" applications based on spin wave transducers, allowing the use of different nanostructured materials with adequate magnetic properties.

Acknowledgements

This work was supported by Postdoctoral Grant from CTIC-UNAM and under projects PAPIIT-UNAM 104513, PAPIT-UNAM IG100314 and CONACYT 194017. In addition, authors wish to thank Dr. Dwight Roberto Acosta Najarro and the Laboratorio Central de Microscopía (LCM)-IFUNAM for providing SEM images.

Notes and references

[a] Fotónica de Microondas, CCADET, Universidad Nacional Autónoma de México (UNAM), Mexico.

[b] Materiales y Nanotecnología, CCADET, Universidad Nacional Autónoma de México (UNAM), Mexico.

1. O. World Health, *WHO guidelines for indoor air quality: selected pollutants*, 2010.
2. S. Agency for Toxic and R. Disease, *Toxicological profile for benzene*, 2007.
3. S. Agency for Toxic and R. Disease, *Toxicological profile for toluene*, 1989.
4. S. Agency for Toxic and R. Disease, *Toxicological profile for xylene*, 1995.
5. A. Ribes, G. Carrera, E. Gallego, X. Roca, M. J. Berenguer and X. Guardino, *Journal of Chromatography A*, 2007, **1140**, 44-55.
6. R. Cumeras, E. Figueras, C. E. Davis, J. I. Baumbach and I. Gracia, *Analyst*, 2015.
7. K. Kim, J. W. Lee and K. S. Shin, *Analyst*, 2013, **138**, 2988-2994.
8. S. Reiß, G. Hagen and R. Moos, *Sensors*, 2008, **8**, 7904-7916.
9. C. H. Lin and C. H. Chen, *Sensors and Actuators, B: Chemical*, 2008, **129**, 531-537.
10. I. Sayago, M. C. Horrillo, S. Baluk, M. Aleixandre, M. J. Fernandez, L. Ares, M. Garcia, J. P. Santos and J. Gutierrez, *Sensors Journal, IEEE*, 2002, **2**, 387-393.
11. B. C. Yadav, A. K. Yadav and A. Kumar, *International Journal of Green Nanotechnology: Biomedicine*, 2012, **4**, 345-353.
12. L. Alwis, T. Sun and K. T. V. Grattan, *Measurement: Journal of the International Measurement Confederation*, 2013, **46**, 4052-4074.
13. J. S. Lee, N. R. Yoon, B. H. Kang, S. W. Lee, S. A. Gopalan, H. M. Jeong, S. H. Lee, D. H. Kwon and S. W. Kang, *Sensors (Switzerland)*, 2014, **14**, 11659-11671.
14. B. Wang, J. C. Cancilla, J. S. Torrecilla and H. Haick, *Nano Letters*, 2014, **14**, 933-938.
15. D. Puglisi, J. Eriksson, C. Bur, A. Schütze, A. L. Spetz and M. Andersson, in *Materials Science Forum*, 2014, vol. 778-780, pp. 1067-1070.
16. D. Matatagui, J. Martí, M. J. Fernández, J. L. Fontecha, J. Gutiérrez, I. Grcia, C. Cané and M. C. Horrillo, *Sensors and Actuators, B: Chemical*, 2011, **154**, 199-205.
17. C. G. Fox and J. F. Alder, *The Analyst*, 1989, **114**, 997-1004.
18. M. Boutamine, A. Bellel, S. Sahli, Y. Segui and P. Raynaud, *Thin Solid Films*, 2014, **552**, 196-203.
19. R. Das, S. Biswas, R. Bandyopadhyay and P. Pramanik, *Sensors and Actuators, B: Chemical*, 2013, **185**, 293-300.
20. J. Kukkola, J. Mäklin, N. Halonen, T. Kyllönen, G. Tóth, M. Szabó, A. Shchukarev, J. P. Mikkola, H. Jantunen and K. Kordás, *Sensors and Actuators, B: Chemical*, 2011, **153**, 293-300.
21. I. Castro-Hurtado, C. Malagù, S. Morandi, N. Pérez, G. G. Mandayo and E. Castaño, *Acta Materialia*, 2013, **61**, 1146-1153.
22. C. Li, D. Zhang, X. Liu, S. Han, T. Tang, J. Han and C. Zhou, *Applied Physics Letters*, 2003, **82**, 1613-1615.
23. G. K. Mor, M. A. Carvalho, O. K. Varghese, M. V. Pishko and C. A. Grimes, *Journal of Materials Research*, 2004, **19**, 628-634.
24. J. Xu, Q. Pan, Y. Shun and Z. Tian, *Sensors and Actuators, B: Chemical*, 2000, **66**, 277-279.
25. J. Zhang, J. Liu, Q. Peng, X. Wang and Y. Li, *Chemistry of Materials*, 2006, **18**, 867-871.
26. E. Ranjith Kumar, R. Jayaprakash, G. Sarala Devi and P. Siva Prasada Reddy, *Sensors and Actuators B: Chemical*, 2014, **191**, 186-191.
27. N. Rezlescu, N. Iftimie, E. Rezlescu, C. Doroftei and P. D. Popa, *Sensors and Actuators B: Chemical*, 2006, **114**, 427-432.
28. S. Wang, X. Gao, J. Yang, Z. Zhu, H. Zhang and Y. Wang, *RSC Advances*, 2014, **4**, 57967-57974.
29. P. Alex, K. M. Reddy, T. Aaron, H. Jason and H. E. Mark, *Nanotechnology*, 2007, **18**, 165502.
30. J. M. Owens, Jr., C. V. Smith, E. P. Snapka and J. H. Collins, Microwave Symposium Digest, 1978 IEEE-MTT-S International, 1978.
31. J. P. Castéra and P. Hartemann, *Circuits Systems and Signal Process*, 1985, **4**, 181-200.
32. R. Marcelli, E. Andreta, G. Bartolucci, M. Cicolani and A. Frattini, *Magnetics, IEEE Transactions on*, 2000, **36**, 3488-3490.
33. K. Horikawa and T. Kodera, Microwave Symposium Digest, 2005 IEEE MTT-S International, 2005.
34. N. Qureshi, O. V. Kolokoltsev, C. L. Ordonez-Romero and G. Lopez-Maldonado, *Journal of Applied Physics*, 2012, **111**, 07A504-507A504-503.
35. D. Matatagui, O. V. Kolokoltsev, N. Qureshi, E. V. Mejía-Uriarte and J. M. Saniger, *Sensors and Actuators B: Chemical*, 2015, **210**, 297-301.
36. B. Issa, I. Obaidat, B. Albiss and Y. Haik, *International Journal of Molecular Sciences*, 2013, **14**, 21266-21305.